Available online at www.sciencedirect.com
ScienceDirect
JOURNAL OF RARE EARTHS, Vol. 33, No. 12, Dec. 2015, P. 1268
JOURNAL OF RARE EARTHS
www.re-journal.com/en/

Enhanced CO oxidation activity of CuO/CeO_2 catalyst prepared by surfactant-assisted impregnation method

SUN Shuaishuai (孙帅帅), MAO Dongsen (毛东森)*, YU Jun (俞 俊)

(Research Institute of Applied Catalysis, School of Chemical and Environmental Engineering, Shanghai Institute of Technology, Shanghai 201418, China)

Received 20 January 2015; revised 8 June 2015

Abstract: A modified CuO/CeO_2 catalyst was prepared by surfactant-assisted impregnation method and showed better catalytic activity for low temperature CO oxidation than that from conventional impregnation method. The physicochemical properties of different CuO/CeO_2 catalysts were characterized by thermogravimetric and differential scanning calorimetric measurements (TG-DSC), X-ray diffraction (XRD), N_2 adsorption-desorption, Raman spectroscopy, H_2 temperature-programmed reduction (H_2-TPR), temperature-programmed desorption of O_2 (O_2-TPD), and diffuse reflectance infrared Fourier transform spectroscopy (DRIFTS). The results suggested that the addition of hexadecyl trimethyl ammonium bromide (CTAB) into the impregnation solution could improve the dispersion of CuO species, which could facilitate Cu^{2+} incorporating into CeO_2 lattice and strengthened the synergistic effects between CuO and CeO_2, making the lattice oxygen more active, and eventually resulting in enhanced activity for CO oxidation.

Keywords: surfactant-assisted impregnation; CuO/CeO_2; CTAB; CO oxidation; rare earths

$CuO\text{-}CeO_2$ mixed oxides have captured tremendous attentions recently because of their low costs, high catalytic activities, and wide applications in CO oxidation[1–10], preferential CO oxidation in H_2-rich stream[11–13], water-gas shift reaction[14,15], combustion of volatile organic compounds[16], NO reduction by CO[17,18] and so on. In particular, the activity of $CuO\text{-}CeO_2$ for low temperature CO oxidation can even be comparable to that of supported Pt catalysts[1,3]. The most frequently used method for the preparation of $CuO\text{-}CeO_2$ catalysts is impregnation[1,2,4,8,10,11,19], because of its simplicity, convenience, and high efficiency[2,20].

The parameters in preparation process of impregnation, such as the metal precursor and content, support, and calcination temperature have significant effects on the physicochemical properties and catalytic activity of the obtained CuO/CeO_2 catalyst. The effect of CuO content and calcination temperature have been studied by Luo et al.[2], and the result show that CuO/CeO_2 catalyst prepared by impregnation method with 15% CuO loading and calcinated under 650 ºC exhibits excellent catalytic activity for CO oxidation. In addition, many attempts also have been made to modify the support CeO_2 to obtain better CuO/CeO_2 catalyst. For example, a series of CeO_2 supports were obtained by Zheng et al.[8,21,22] via sol-gel, alcoholthermal, and thermal decomposition methods, and found that CeO_2 with smaller particle sizes, better crystallinity, and larger surface areas led to the formation of more highly dispersed CuO species responsible for high activity in CO oxidation. In another work, Gamarra et al.[13] synthesized CeO_2 nanocubes, nanorods, and nanospheres by hydrothermal, microemulsion, and precipitation methods, respectively, and found that the CuO/CeO_2 nanocubes exhibited the highest activity in CO oxidation due to the highly dispersed CuO and the strong interaction between CuO and the (100) faces of CeO_2 support.

Therefore, it can be concluded from the previous studies that, enhanced catalytic activity for CO oxidation can be obtained by promoting the CuO dispersion and strengthening the synergistic effects between CuO and CeO_2[1,5,9,13,19]. Considering the results, some studies captured our attention. Shen et al.[23] found that catalyst prepared by ammonia coordination-impregnation method possesses a higher dispersion and lower-temperature reducibility of copper phase. On the other hand, hexadecyl trimethyl ammonium bromide (CTAB) usually works as a capping agent to tune the crystal size of many metals and metal-organic frameworks (MOFs)[24,25]. Hence, we considered that the surfactant-assisted impregnation method by adding CTAB into the impregnation solution of copper nitrate may also play a role in improving the CuO dispersion on CuO/CeO_2 catalyst.

Herein, two kinds of CuO/CeO_2 catalysts were prepared by surfactant-assisted impregnation method with the addition of CTAB in the impregnation solution and

Foundation item: Project supported by the National Natural Science Foundation of China (21273150) and ''Shu Guang'' Project (10GG23) of Shanghai Municipal Education Commission and Shanghai Education Development Foundation

* **Corresponding author:** MAO Dongsen (**E-mail:** dsmao@sit.edu.cn; **Tel.:** +86-21-6087 3625)

DOI: 10.1016/S1002-0721(14)60556-1

conventional impregnation method, respectively. The influences of the modified impregnation method on the dispersion and redox property of the obtained CuO as well as the synergistic effects between CuO and CeO_2 were systematically investigated. CO oxidation was used as a probe reaction to compare the catalytic activity of the different CuO/CeO_2 catalysts.

1 Experimental

1.1 Catalyst preparation

All chemicals were of analytical grade from Sinopharm Chemical Reagent Co., Ltd. (China) and used without further purification. The modified CuO/CeO_2 catalyst was prepared by impregnating a commercial CeO_2 support (S_{BET}=11.1 m^2/g) with an aqueous solution of CTAB and a calculated amount of $Cu(NO_3)_2{\cdot}3H_2O$ to obtain a Cu loading of 10 wt.%. The amount of CTAB was $n_{(CTAB)}$:$n_{(Cu)}$=2% determined by its dissolvability in water. CeO_2 support was pretreated at 120 ºC for 4 h before use to remove the impurity adsorbed on the surface. After being impregnated quiescently at room temperature (RT) for 24 h, the sample was dried at 90 ºC for 20 h, followed by calcination in static air at 500 ºC for 4 h. The prepared catalyst was denoted as Cu/Ce(SI). For comparison, CuO/CeO_2 catalyst prepared by conventional impregnation method without the addition of CTAB was also synthesized and donated as Cu/Ce(CI).

1.2 Catalyst characterization

Simultaneous thermogravimetric and differential scanning calorimetric measurements (TG-DSC) were carried out on a NETZSCH STA 449-F3 thermal analyzer made in Germany. The experiments were performed under an air stream of 50 mL/min from 30 to 500 ºC at a heating rate of 10 ºC/min and then hold at this temperature for another 4 h.

Powder X-ray diffraction (XRD) patterns were recorded on a PANalytical X'Pert instrument using Ni-filtered Cu Kα radiation (λ=0.15406 nm) at 40 kV and 40 mA. Two theta angles ranged from 10 º to 90 º with a scanning rate of 6 (º)/min. The crystallite size of CuO was calculated from the XRD patterns using the Scherrer equation. The cell parameter values were calculated by standard cubic indexation method using the intensity of the CeO_2 (111) peak.

N_2 adsorption-desorption isotherms were obtained at –196 ºC on a Micrometrics ASAP-2020 adsorption apparatus, after all samples were degassed under vacuum at 300 ºC for 10 h. The specific surface areas (S_{BET}) were calculated from the linear part of the Braunauer-Emmett-Teller (BET) plot.

Raman spectra (at 4 cm^{-1} resolution) were obtained with a DXR-Raman microscope (Thermo Fisher Scientific, American) using the 532 nm exciting line (20 mW beam), 5 scans for every spectrum.

H_2 temperature-programmed reduction (H_2-TPR) was carried out in a quartz micro-reactor. Firstly, 20 mg of the as-prepared sample was pretreated at 400 ºC in N_2 stream for 1 h before the TPR measurement. Then the sample was heated to 500 ºC at a rate of 10 ºC/min under a flow of H_2 (10 vol.%)/N_2 (50 mL/min). The effluent gas was analyzed by an on-line GC equipped with a thermal conductivity detector (TCD). Before the TPR test, the reducing gas H_2 (10 vol.%)/N_2 (50 mL/min) was directly introduced into the GC system for 10 min, then the H_2 consumption for per unit area can be obtained from the amount of introduced H_2 and the integral peak area. In this way, the actual H_2 consumption of different samples during the TPR test can be calculated by integrating the area of the reduction peak.

O_2-TPD was performed on the same equipment as used in TPR test. 100 mg catalyst was pretreated under He flow (50 mL/min) with the temperature ramping from 25 to 500 ºC at a rate of 10 ºC/min, and then held at 500 ºC for 1 h before being cooled down to RT in He flow. The next step was O_2 adsorption at RT for 1 h, and then the gas was swept again with He for 2 h at 50 ºC. Subsequently, the sample was heated in flowing He (50 mL/min) up to 500 ºC at a rate of 10 ºC/min, while the desorbed species was detected with a quadrupole mass spectrometer (QMS, Balzers OmniStar 200).

In situ diffuse reflectance infrared Fourier transform spectroscopy (DRIFTS) data were collected using a Nicolet 6700 FT-IR spectrometer fitted with a MCT detector. The DRIFTS cell (Harrick) was fitted with CaF_2 windows and a heating cartridge that allowed samples to be heated to 400 ºC. The sample in the cell was pretreated in N_2 at 400 ºC for 1 h, and then the backgrounds corresponding to different temperatures were scanned in the cooling process. After the sample being cooled to 30 ºC, the reaction mixture (4 vol.% CO, 10 vol.% O_2, balance in N_2, total flow rate=30 mL/min) was introduced and the IR spectrum of CO adsorbed on the catalyst was recorded. When the saturated adsorption of CO was achieved, the sample was heated to the next temperature. The spectral resolution was 4 cm^{-1} and the number of scans was 64.

1.3 Catalytic activity tests

Prior to the catalytic measurements, the catalyst was pretreated in a N_2 stream (50 mL/min) under 200 ºC for 1 h to remove the impurities, and then cooled to RT. The CO oxidation activities of the catalysts were measured in a fixed micro-reactor (6 mm i.d.) under atmospheric pressure with a gas composition of 4 vol.% CO, 10 vol.% O_2 and 86 vol.% N_2 at a space velocity of 9,000 mL/(g·h). 200 mg catalyst was used for each measurement and was sieved to 40–60 mesh so that pressure drop, concentration and temperature gradients over the catalyst bed

could be negligible. The temperature of the catalyst bed is measured by a thermocouple placed in a tube coaxial with the reactor. The products were analyzed by an online GC equipped with a flame ionization detector (FID). To allow for the detection of CO and CO_2 with FID, a methanator was inserted between one GC column and the FID.

2 Results and discussion

2.1 Testing of catalytic activity

The activities of different CuO/CeO_2 catalysts for CO oxidation are shown in Fig. 1. It can be seen that the Cu/Ce(SI) catalyst prepared by surfactant-assisted impregnation method shows a higher catalytic activity than the Cu/Ce(CI) catalyst prepared by conventional impregnation method in the whole temperature range analyzed; T_{99} (the temperature for 99% CO conversion) on it is about 120 ºC, while that on Cu/Ce(CI) catalyst reaches 140 ºC. Especially when the catalytic reaction takes place at 80 ºC, the CO conversion on Cu/Ce(SI) and Cu/Ce(CI) is 65% and 54%, respectively. Thus, the modified impregnation method has a significant effect on improving the activity of CuO/CeO_2 catalyst for low temperature CO oxidation.

2.2 Thermal behaviors of the sample

The residual CTAB on Cu/Ce(SI) catalyst surface may play a negative role for the catalytic activity by covering the active sites; therefore, it is necessary to make sure whether some CTAB are still existing after the dried samples calcined under static air at 500 ºC for 4 h. Neither weight loss nor thermal effect can be observed on the TG-DSC curves of Cu/Ce(SI) catalyst (not shown), suggesting that no CTAB exists on the obtained Cu/Ce(SI) catalyst.

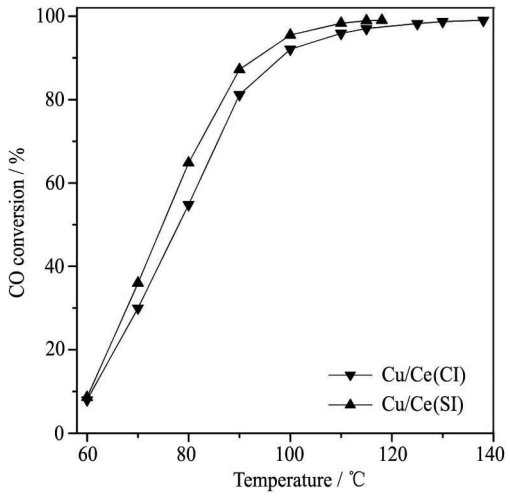

Fig. 1 CO oxidation activity over Cu/Ce(CI) and Cu/Ce(SI) catalysts

Reaction conditions: 4 vol.% CO, 10 vol.% O_2, balance in N_2, SV=9,000 mL/(g·h)

2.3 XRD and BET surface area

Fig. 2 exhibits the XRD patterns of pure CeO_2 and CuO/CeO_2 catalysts. No CeO_2 phase other than cubic CeO_2 can be observed for all of these samples, indicating that the heating process at 500 ºC has a negligible effect on the crystal form of support CeO_2. When CuO (10 wt.%) is loaded onto CeO_2, characteristic peaks assigned to CuO at 35.5º and 38.7º appear on all CuO/CeO_2 catalysts, suggesting that bulk CuO has been formed either on Cu/Ce(CI) catalyst prepared by conventional impregnation method or on Cu/Ce(SI) catalyst prepared by surfactant-assisted impregnation method.

Table 1 summarizes the CuO crystallite size calculated by the Scherrer equation on different CuO/CeO_2 samples. It is clear that, the CuO crystallite size on Cu/Ce(SI) catalyst (18 nm) is significantly smaller than that on Cu/Ce(CI) catalyst (26 nm), suggesting that the surfactant-assisted impregnation method can inhibit the growth of CuO bulk during the sample preparation. The reason may be that the long hydrophobic hydrocarbon chain of CTAB binds to the surface of the seeds for CuO precursors in aqueous solution and acts as capping agents to slow down the crystal growth in the crystallization process[24,25]. As a consequence, the smaller seeds lead to the formation of smaller particles of CuO. Even though the amount of CTAB used in our study is limited, the significant role of it has been reflected consistent with the result of Pan et al.[25], who found that the addition of 0.0025 wt.% CTAB to the synthesis solution can have an influence on decreasing the mean particle size of ob-

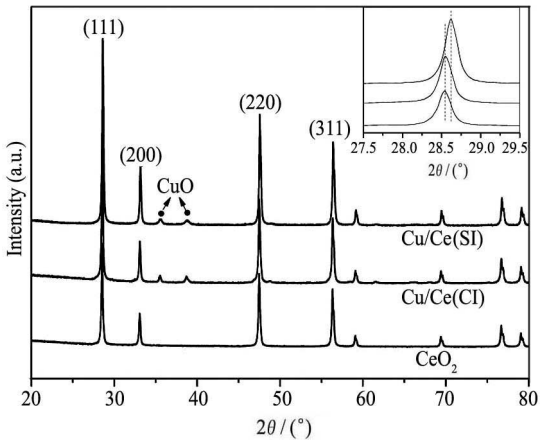

Fig. 2 XRD patterns of CeO_2 and different CuO/CeO_2 catalysts

Table 1 BET surface area, grain size, lattice parameter and full width at half maximum (FWHM) of F_{2g} vibration band of different samples

Sample	S_{BET}/ (m^2/g)	D_{CuO}*/ nm	Lattice parameter/nm	FWHM / cm^{-1}
CeO_2	11.0	–	0.5414	11
Cu/Ce(CI)	8.7	26	0.5412	13
Cu/Ce(SI)	9.7	18	0.5401	19

* The particle size of CuO is the average value of the calculated values based on CuO (002) and CuO (111)

tained material. Additionally, Cu/Ce(SI) catalyst exhibits a larger BET surface area than Cu/Ce(CI) catalyst; this result is related to the better CuO dispersion resulting from the smaller CuO size and may be one of the reasons that Cu/Ce(SI) catalyst possesses the higher catalytic activity, because the catalyst with higher surface area can provide more active site for CO oxidation[26].

On the other hand, it can be seen from the inset in Fig. 2 that the diffraction peak of CeO_2(111) on Cu/Ce(SI) catalyst shifts to a higher angle compared with that on pure CeO_2 and Cu/Ce(CI) catalyst. This phenomenon suggests that lattice constriction (the lattice parameter of CeO_2 on different samples is shown in Table 1) has taken place on Cu/Ce(SI) catalyst prepared by surfactant-assisted impregnation method. According to previous studies[7,14,15], the lattice constriction on CuO/CeO_2 catalyst may be due to the Cu^{2+} ions (0.072 nm) incorporating into CeO_2 lattice and substituting the Ce^{4+} (0.097 nm) to form the Cu–O–Ce solid solution. The generated Cu–O–Ce solid solution has two roles in CO oxidation: on one hand, it can promote the CO adsorbing on the catalyst surface (Cu^{+}); on the other hand, it can improve the redox properties of the catalyst. Both factors are beneficial to enhancing the activity of CuO/CeO_2 catalyst[19]. The smaller lattice parameter on Cu/Ce(SI) catalyst (0.5401 nm) indicates that more Cu^{2+} ions have incorporated into the CeO_2 lattice to form the Cu–O–Ce solid solution, which may result from the better CuO dispersion and is responsible for its higher catalytic activity.

2.4 Raman analysis

Raman analysis is a potential tool to obtain additional structural information of CuO/CeO_2 sample, because it is sensitive to the crystalline symmetry and oxygen lattice vibrations[27] in contrast to the XRD result. The Raman spectra of support CeO_2 and different CuO/CeO_2 catalysts are shown in Fig. 3. A strong peak at about 465 cm^{-1}, corresponding to the F_{2g} Raman vibration mode of fluorite CeO_2[12,13,19,28], can be observed on all samples.

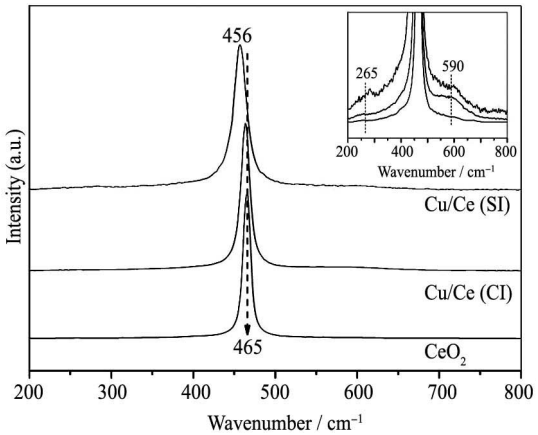

Fig. 3 Raman spectra for CeO_2 and CuO/CeO_2 catalysts prepared by different methods

Once CuO is introduced, two new peaks at about 265 and 590 cm^{-1} appear on the CuO/CeO_2 catalysts (inset in Fig. 3). The weak band at 265 cm^{-1} is attributed to the displacement of oxygen atoms from their ideal fluorite lattice positions[12], and the broad band at 590 cm^{-1} is often related to the presence of oxygen vacancies in the CeO_2 lattice caused by the incorporation of Cu^{2+} into CeO_2 lattice, which must be accompanied by formation of oxygen vacancies for charge balance ($Ce^{4+}+O^{2-}\leftrightarrow Cu^{2+}+V_{\ddot{O}}$; $V_{\ddot{O}}$ being a doubly ionized oxygen vacancy)[13,19,26]. No obvious peaks linked to CuO can be found on the Raman spectra of the CuO/CeO_2 catalysts. It may be due to the fact that the Raman diffuse reflection of CuO is too weak to be distinguished under this scale; similar phenomenon was also observed by Li et al.[12].

The relative concentration of oxygen vacancies on different catalysts is usually calculated from the area ratio of peaks at 590 and 465 cm^{-1} (A_{590}/A_{465})[9,12]. However, the intensity of peak at 590 cm^{-1} is too weak to accurately achieve the A_{590}/A_{465} in our study. So, it is unworkable to obtain the relative concentration of oxygen vacancies on different catalysts from the peak at 590 cm^{-1}. Nevertheless, it is worth noticing that a small red shift and broadening of the F_{2g} band (FWHM, Table 1) can be observed on Cu/Ce(SI) catalyst compared with pure CeO_2. According to the literatures[12,28,29], this phenomenon also acts as an evidence of the incorporation of copper into ceria lattice and the generation of oxygen vacancies, which induce the CeO_2 lattice to distort. Therefore, from the shift and broadening extent of the F_{2g} band (shown in Table 1), it can be inferred that more oxygen vacancies have been generated on Cu/Ce(SI) catalyst, consistent with the microstrain values obtained from XRD analysis. The reaction mechanism of CO oxidation on CuO/CeO_2 system is proposed to involve a redox reaction involving lattice oxygen and oxygen vacancies[12,29]. Therefore, the relative higher intensity of oxygen vacancies on Cu/Ce(SI) catalyst may make an important contribution to its better catalytic activity[12,19].

2.5 H_2-TPR

H_2-TPR experiments were conducted to investigate the reduction properties of CuO/CeO_2 catalysts. From the inset in Fig. 4, it can be seen that CuO obtained by thermal decomposition of copper nitrate at 500 ºC for 4 h shows a single reduction peak at around 260 ºC, attributed to the complete reduction of Cu^{2+} to Cu^0; CeO_2 has two reduction peaks at about 565 and 860 ºC, ascribed to the reduction of surface and bulk oxygen species, respectively[30].

Fig. 4 displays the H_2-TPR curves of CuO/CeO_2 catalysts prepared by different methods. Four reduction peaks can be seen on the H_2-TPR curve of the Cu/Ce(SI) catalyst, the former three peaks at lower temperatures corresponding to three different types of copper species

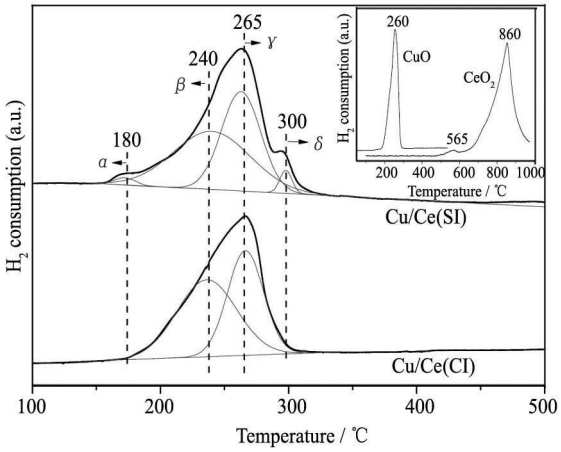

Fig. 4 H_2-TPR curves for CuO/CeO_2 catalysts prepared by different methods

entities differing in their degree of interaction with the support CeO_2[2,12,13,19]. More specifically, peak α (180 ºC) is ascribed to the reduction of finely dispersed copper species strongly interacting with the CeO_2 support; peak β (240 ºC) is assigned to the reduction of larger particles of copper species; peak γ (265 ºC) is attributed to the reduction of bulk copper species interacting weakly with the CeO_2 support[13,19]. The higher temperature peak at about 300 ºC (peak δ) is related to the reduction of Cu^{2+} in CeO_2 lattice, which is proposed to be the most difficult to reduce[13,28]. However, only two reduction peaks assigned to larger CuO particles and bulk CuO can be observed on the H_2-TPR curve of the Cu/Ce(CI) catalyst.

In addition, a quantitative attribution of the TPR peaks to different species has been calculated and the results are shown in Table 2. It is clear that there are 2% of CuO which is finely dispersed and another 3% of Cu^{2+} which has incorporated into CeO_2 lattice on Cu/Ce(SI) catalyst. This result further indicates that the addition of CTAB can improve the dispersion of CuO and facilitate Cu^{2+} incorporating into CeO_2 lattice, in agreement with the results obtained from XRD and Raman analyses. On the other hand, the H_2 uptake is calculated by integrating the area of the reduction peak. During the TPR test up to 500 ºC, the actual H_2 consumption of CuO/CeO_2 catalysts is higher than that required for full reduction of copper species, indicating that surface ceria reduction must also contribute to the observed reduction peaks. According to previous study, stronger synergistic effects between CuO and CeO_2 are believed to enhance their individual reducibility[9,30]. Thus, the larger amount of excess H_2 uptake (134 μmol/g) achieved on Cu/Ce(SI) catalyst suggests more active lattice oxygen and stronger synergistic effects on it, which may contribute to the higher catalytic activity[9].

Table 2 Results of H_2-TPR analysis

Sample	Reduction temperature/ºC (relative intensities/%)*				Total H_2 consumption/	Excess H_2 consumption/
	α	β	γ	δ	(μmol/g)	(μmol/g)
Cu/Ce(CI)	–	236 (55)	266 (45)	–	1289	64
Cu/Ce(SI)	180 (2)	231 (51)	263 (44)	298 (3)	1359	134

* The data in parentheses represent the percentage of the respective peak area in total area

2.6 O_2-TPD

O_2-TPD is a good technique to provide more information about the lattice oxygen and oxygen vacancies. The O_2-TPD profiles of the Cu/Ce catalysts prepared by different methods are shown in Fig. 5. In the temperature range, an O_2 desorption peak at about 325 ºC can be observed on Cu/Ce(SI), while it is invisible on Cu/Ce(CI). According to the literatures[31,32], this peak is attributed to the surface chemically adsorbed oxygen species, which shows more mobility than the bulk lattice O^{2-} species and is indispensable for the superior catalytic activity of CuO-CeO_2 catalyst for CO oxidation. So, Cu/Ce(SI) with larger amounts of surface adsorbed oxygen species resulting from plentiful surface oxygen vacancy[32] shows better reducibility (more excess H_2 consumption in H_2-TPR analysis) and catalytic activity for CO oxidation.

2.7 *In situ* DRIFTS study

In situ DRIFTS experiments were conducted to further investigate the influence of different impregnation methods on the CO adsorption property of CuO/CeO_2 catalysts. As shown in Fig. 6, both Cu/Ce(CI) and Cu/Ce(SI) show a strong peak at about 2105 cm^{-1}, assigning to the linear CO chemisorbed on Cu^+ sites (Cu^+–CO)[9,12,19,33], and a series peaks related to formate, carbonate or carboxylate species absorbed on catalyst surface in the wavenumber region of 1000–1700 cm^{-1}.

In particular, when the spectra was collected at 30 ºC, the intensity of the Cu^+–CO band on Cu/Ce(CI) catalyst is about two times weaker than that on Cu/Ce(SI) catalyst. This could be caused by the absence of highly dis-

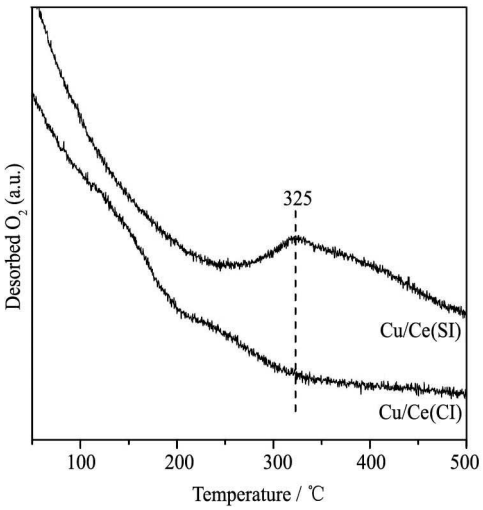

Fig. 5 O_2-TPD profiles of CuO/CeO_2 catalysts prepared by different methods

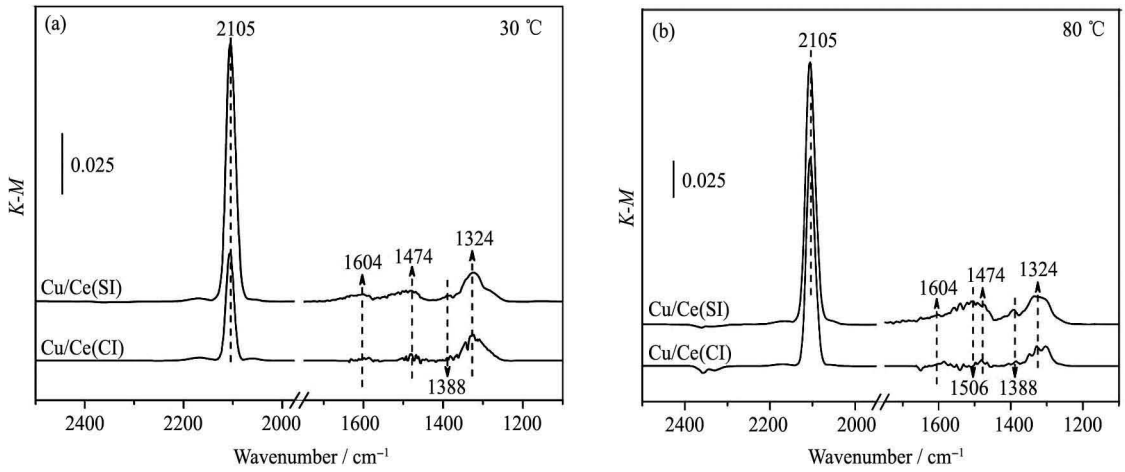

Fig. 6 DRIFTS spectra for different CuO/CeO_2 catalysts recorded at 30 ºC (a) and 80 ºC (b) after introducing the reaction mixtures (4 vol.% CO, 10 vol.% O_2, balance in N_2, total flow rate=30 mL/min)

persed CuO, which is probably as the origin of Cu^+ under the stronger synergistic effects[19]. Additionally, as shown in Fig. 6(b), a broad band at about 1506 cm^{-1}, attributed to inorganic carboxylate species resulted from CO_2 interacted with CeO_2 surface[34], can be observed obviously on Cu/Ce(SI) catalyst, while it is invisible on Cu/Ce(CI) catalyst. This phenomenon indicates that noticeable amounts of CO_2 have been generated on Cu/Ce(SI) catalyst at 80 ºC as a consequence of its excellent catalytic activity at this temperature.

3 Conclusions

In summary, we successfully prepared a modified CuO/CeO_2 catalyst by the surfactant-assisted impregnation method, which exhibited better catalytic activity than that from conventional impregnation method. The higher activity was mainly due to the improved dispersion of CuO through the addition of CTAB into the impregnation solution. The highly dispersed CuO could provide active sites (Cu^+) for CO adsorption and facilitated Cu^{2+} incorporating into CeO_2 lattice to form Cu–O–Ce solid solution, which made the lattice oxygen more active.

References:

[1] Liu W, Flytzani-Stephanopoulos M. Total oxidation of carbon oxide and methane over transition metal-fluorite oxide composite catalysts. I. Catalyst composition and activity. *J. Catal.*, 1995, **153**: 304.

[2] Luo M F, Zhong Y J, Yuan X X, Zheng X M. TPR and TPD studies of CuO/CeO_2 catalysts for low temperature CO oxidation. *Appl. Catal. A: Gen.*, 1997, **162**: 121.

[3] Tschöpe A, Schaadt D, Birringer R, Ying J Y. Catalytic properties of nanostructured metal oxides synthesized by inert gas condensation. *Nanostruct. Mater.*, 1997, **9**: 423.

[4] Jiang X Y, Lu G L, Zhou R X, Mao J X, Chen Y, Zheng X M. Studies of pore structure, temperature-programmed reduction performance, and micro-structure of CuO/CeO_2 catalysts. *Appl. Surf. Sci.*, 2001, **173**: 208.

[5] Sedmak G, Hočevar S, Levec J. Transient kinetic model of CO oxidation over a nanostructured $Cu_{0.1}Ce_{0.9}O_{2-y}$ catalyst. *J. Catal.*, 2004, **222**: 87.

[6] Tang X L, Zhang B C, Li Y, Xu Y D, Xin Q, Shen W J. Carbon monoxide oxidation over CuO/CeO_2 catalysts. *Catal. Today*, 2004, **93-95**: 191.

[7] Martínez-Arias A, Hungría A B, Fernández-García M, Conesa J C, Munuera G. Interfacial redox processes under CO/O_2 in a nanoceria-supported copper oxide catalyst. *J. Phys. Chem. B*, 2004, **108**: 17983.

[8] Zheng X C, Wu S H, Wang S P, Wang S R, Zhang S M, Huang W P. The preparation and catalytic behavior of copper-cerium oxide catalysts for low-temperature carbon monoxide oxidation. *Appl. Catal. A: Gen.*, 2005, **283**: 217.

[9] Qi L, Yu Q, Dai Y, Tang C J, Liu L J, Zhang H L, Gao F, Dong L, Chen Y. Influence of cerium precursors on the structure and reducibility of mesoporous $CuO-CeO_2$ catalysts for CO oxidation. *Appl. Catal. B: Environ.*, 2012, **119-120**: 308.

[10] Mao D S, Tao L H, Wang Q, Guo Y L, Lu G Z. Low temperature oxidation of CO over $CuO-CeO_2$ catalyst prepared by solid-state chemical reaction. *Chin. J. Inorg. Chem.* (in Chin.), 2010, **26**: 447.

[11] Avgouropoulos G, Ioannides T, Matralis H. Influence of the preparation method on the performance of $CuO-CeO_2$ catalysts for the selective oxidation of CO. *Appl. Catal. B: Environ.*, 2005, **56**: 87.

[12] Li J, Han Y X, Zhu Y H, Zhou R X. Purification of hydrogen from carbon monoxide for fuel cell application over modified mesoporous $CuO-CeO_2$ catalysts. *Appl. Catal. B: Environ.*, 2011, **108-109**: 72.

[13] Gamarra D, López Cámara A, Monte M, Rasmussen S B, Chinchilla L E, Hungría A B, Munuera G, Gyorffy N, Schay Z, Cortés Corberán V, Conesa J C, Martínez-Arias A. Preferential oxidation of CO in excess H_2 over CuO/CeO_2 catalysts: characterization and performance as a function of the exposed face present in the CeO_2 support. *Appl. Catal. B: Environ.*, 2013, **130-131**: 224.

[14] Djinović P, Batista J, Pintar A. Calcination temperature

and CuO loading dependence on CuO-CeO_2 catalyst activity for water-gas shift reaction. *Appl. Catal. A: Gen.*, 2008, **347**: 23.

[15] Si R, Raitano J, Yi N, Zhang L H, Chan S W, Flytzani-Stephanopoulos M. Structure sensitivity of the low-temperature water-gas shift reaction on Cu-CeO_2 catalysts. *Catal. Today*, 2012, **180**: 68.

[16] Delimaris D, Ioannides T. VOC oxidation over CuO-CeO_2 catalysts prepared by a combustion method. *Appl. Catal. B: Environ.*, 2009, **89**: 295.

[17] Yao X J, Xiong Y, Sun J F, Gao F, Deng Y, Tang C J, Dong L. Influence of MnO_2 modification methods on the catalytic performance of CuO/CeO_2 for NO reduction by CO. *J. Rare Earths*, 2014, **32**: 131.

[18] Gu X R, Li H, Liu L C, Tang C J, Gao F, Dong L. Promotional effect of CO pretreatment on CuO/CeO_2 catalyst for catalytic reduction of NO by CO. *J. Rare Earths*, 2014, **32**: 139.

[19] Jia A P, Hu G S, Meng L, Xie Y L, Lu J Q, Luo M F. CO oxidation over CuO/$Ce_{1-x}Cu_xO_{2-\delta}$ and $Ce_{1-x}Cu_xO_{2-\delta}$ catalysts: synergetic effects and kinetic study. *J. Catal.*, 2012, **289**: 199.

[20] Manzoli M, Di Monte R, Boccuzzi F, Coluccia S, Kašpar J. CO oxidation over CuO_x-CeO_2-ZrO_2 catalysts: transient behaviour and role of copper clusters in contact with ceria. *Appl. Catal. B: Environ.*, 2005, **61**: 192.

[21] Zheng X C, Wang S P, Wang S R, Zhang S M, Huang W P, Wu S H. Copper oxide catalysts supported on ceria for low-temperature CO oxidation. *Catal. Commun.*, 2004, **5**: 729.

[22] Zheng X C, Zhang X L, Wang X Y, Wang S R, Wu S H. Preparation and characterization of CuO/CeO_2 catalysts and their applications in low-temperature CO oxidation. *Appl. Catal. A: Gen.*, 2005, **295**: 142.

[23] Shen Y X, Lu G Z, Guo Y, Wang Y Q. A synthesis of high-efficiency Pd-Cu-Cl_x/Al_2O_3 catalyst for low temperature CO oxidation. *Chem. Commun.*, 2010, **46**: 8433.

[24] Niu W X, Zheng S L, Wang D W, Liu X Q, Li H J, Han S, Chen J A, Tang Z Y, Xu G B. Selective synthesis of single-crystalline rhombic dodecahedral, octahedral, and cubic gold nanocrystals. *J. Am. Chem. Soc.*, 2009, **131**: 697.

[25] Pan Y C, Heryadi D, Zhou F, Zhao L, Lestari G, Su H B, Lai Z P. Tuning the crystal morphology and size of zeolitic imidazolate framework-8 in aqueous solution by surfactants. *CrystEngComm.*, 2011, **13**: 6937.

[26] Luo M F, Ma J M, Lu J Q, Song Y P, Wang Y J. High-surface area CuO-CeO_2 catalysts prepared by a surfactant-templated method for low-temperature CO oxidation. *J. Catal.*, 2007, **246**: 52.

[27] Fernández-García M, Martínez-Arias A, Iglesias-Juez A, Belver C, Hungría A B, Conesa J C, Soria J. Structural characteristics and redox behavior of CeO_2-ZrO_2/Al_2O_3 supports. *J. Catal.*, 2000, **194**: 385.

[28] McBride J R, Hass K C, Poindexter B D, Weber W H. Raman and X-ray studies of $Ce_{1-x}RE_xO_{2-y}$, where RE=La, Pr, Nd, Eu, Gd, and Tb. *J. Appl. Phys.*, 1994, **76**: 2435.

[29] Liu Y, Wen C, Guo Y, Lu G Z, Wang Y Q. Modulated CO oxidation activity of M-doped ceria (M=Cu, Ti, Zr, and Tb): Role of the Pauling electronegativity of M. *J. Phys. Chem. C*, 2010, **114**: 9889.

[30] Zimmer P, Tschöpe A, Birringer R. Temperature-programmed reaction spectroscopy of ceria- and Cu/ceria-supported oxide catalyst. *J. Catal.*, 2002, **205**: 339.

[31] Chen Y N, Liu D S, Yang L J, Meng M, Zhang J, Zheng L R, Chu S Q, Hu T D. Ternary composite oxide catalysts CuO/Co_3O_4-CeO_2 with wide temperature-window for the preferential oxidation of CO in H_2-rich stream. *Chem. Eng. J.*, 2013, **234**: 88.

[32] He C, Yu Y K, Shen Q, Chen J S, Qiao N L. Catalytic behavior and synergistic effect of nanostructured mesoporous CuO-MnO_x-CeO_2 catalysts for chlorobenzene destruction. *Appl. Surf. Sci.*, 2014, **297**: 59.

[33] Bera P, Cámara A L, Hornés A, Martínez-Arias A. Comparative in situ DRIFTS-MS study of ^{12}CO- and ^{13}CO-TPR on CuO/CeO_2 catalyst. *J. Phys. Chem. C*, 2009, **113**: 10689.7

[34] Li C, Sakata Y, Arai T, Domen K, Maruya K, Onishi T. Carbon monoxide and carbon dioxide adsorption on cerium oxide studied by Fourier-transform infrared spectroscopy. Part 1. Formation of carbonate species on dehydroxylated CeO_2 at room temperature. *J. Chem. Soc., Faraday Trans.*, 1989, **85**: 929.